Supporting information

Solution-processable Double-boron-nitrogen-doped Deep Blue Multi-resonance Thermally Activated Delayed Fluorescence Materials

Hengxuan Qi[ab], Jianxing Chen[c], Deli Li[d], Ziru Xin[b], Jiasen Zhang[b], Chao Xia[b], Wenjun Wang[*a], Ruixiang Peng[*b], Lin Wu[*b], Xiugang Wu*[c], Wei Li*[b], and Ziyi Ge*[b]

[a.]School of Physical Science and Information Technology, Liaocheng University, Liaocheng 2520259, P. R. China. E-mail: phywwang@163.com

[b.]Zhejiang Provincial Engineering Research Center of Energy Optoelectronic Materials and Devices, Ningbo Institute of Materials Technology and Engineering, Chinese Academy of Sciences, Ningbo, 315201, P. R. China.Center of Materials Science and Optoelectronics Engineering, University of Chinese Academy of Sciences, P. R. China. E-mail:pengrx@nimte.ac.cn;wulin@nimte.ac.cn; liwei1987@nimte.ac.cn; geziyi@nimte.ac.cn.

[c.]School of Materials Science and Engineering, Jiangsu Engineering Laboratory of Light-Electricity-Heat Energy-Converting Materials and Applications, Changzhou University, Changzhou 213164, China Email: xgwu16@cczu.edu.cn.

[d.]Institute for Smart Materials & Engineering, University of Jinan, No. 336 Nanxinzhuang West Road, Jinan, 250022, P. R. China

Corresponding Author

*[a]Email: phywwang@163.com
*[b]Email: pengrx@nimte.ac.cn; wulin@nimte.ac.cn; liwei1987@nimte.ac.cn; geziyi@nimte.ac.cn
*[c]Email: xgwu16@cczu.edu.cn

1. General Information

The ^{1}H NMR spectra were recorded on Bruker NMR spectrometers operating at 400 and 151 MHz. Mass spectra were recorded by AB Sciex TripleTOF 4600 mass analyzer (AB Sciex, Framingham, MA, USA). UV-vis spectra were recorded using Perkin-Elmer Lambda 950-PKA UV-Vis. All the low-temperature steady-state fluorescence and phosphorescence spectra were recorded by (Horiba Jobin Yvon) FluoroMax-4 Spectro-fluorometer with a Dewar flask. Low-temperature fluorescence spectra can be measured using stable-state fluorescence mode without time delay. Low-temperature phosphorescence spectra can be recorded using phosphorescence mode after a time delay of 0.05-50 ms (delay time adjustment range: 50 μs–100 ms) to eliminate the influence of low-temperature fluorescence spectra. Cyclic voltammetry measurements were conducted using the electrochemical workstation Multiautolab M204. Photoluminescence quantum yields (PLQYs) in doped films were measured utilizing an integrating sphere of Hamamatsu absolute PLQY spectrometer (C11347-01). Thermogravimetric analyses (TGA) were conducted on a Netzsch TGA 2019F1, and differential scanning calorimetry (DSC) measurements were carried out on a Netzsch DSC 214. Both TGA and DSC measurements were under N_2 flow.

1.1. Quantum Chemical Method

All simulations were performed using the Gaussian 16 program package [1]. The ground-state (S_0) geometries were optimized for all the investigated molecules using the B3LYP functional with the 6-31G* basis set in vacuum, using the initial guess. The excited state was optimized using TD-DFT/M06-2X/6-31G* in toluene with a polarizable continuum model (PCM).[2] Frontier molecular orbitals (FMOs), natural transition orbitals (NTOs), and root-mean-square displacements (RMSDs) were further analyzed using the wavefunction analyzers Multiwfn and VMD, with results calculated using the Gaussian 16 program.[3]

1.2. Device Fabrication and Characterization

Glass substrates pre-coated with a 95-nm-thin layer of indium tin oxide (ITO) with a sheet resistance of 10 Ω per square was thoroughly cleaned in an ultrasonic bath of tetrahydrofuran, isopropyl alcohol, detergent, deionized water, and isopropyl alcohol and was then treated with O2 plasma for 5 minutes in sequence. Organic layers were deposited onto the ITO-coated glass substrates by thermal evaporation under a high vacuum (~10^{-5} Pa). The cathode was patterned using a shadow mask with 3 mm x 3 mm openings. Deposition rates are 1 − 2 Å s^{-1} for organic materials and 2 - 5 Å s^{-1} for aluminum, respectively. The current density, luminance versus driving voltage characteristics, and EL spectra were measured by Keithley 2400 and Konica Minolta CS2000 chromameter. EQEs were automatically estimated from the current density, brightness, and

EL spectra, assuming a Lambertian distribution.

2. Synthetic procedures

All the reagents were purchased from the *Casmart Reagent* Platform or *Bidepharm* and used as received without further purification. The target molecules' intermediates were synthesized via a one-step, common palladium-catalyzed Buchwald-Hartwig reaction. The target molecules were synthesized via one-step common borylation reactions. The synthetic procedures are detailed below.

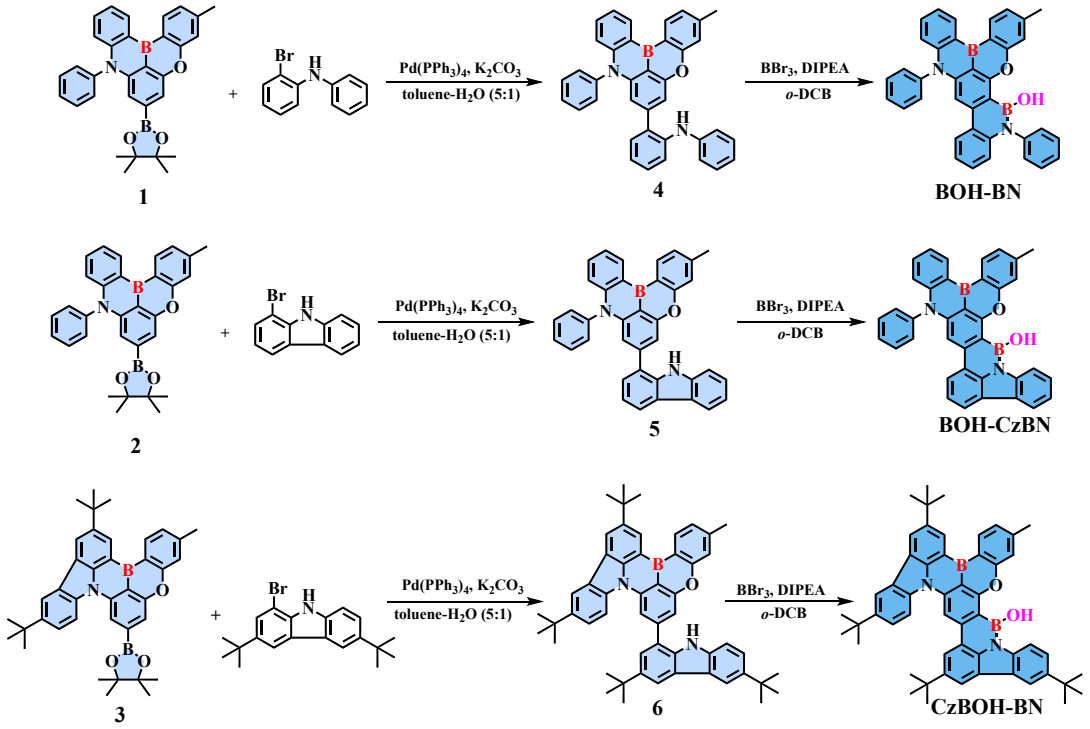

Scheme1. Detailed synthesis procedures for BOH-BN, BOH-CzBN, and CzBOH-BN, respectively.

Synthesis of Compound 1: In a 250 mL flask charged with argon,3-methyl-9-phenyl-7-(4,4,5,5-tetra methyl-1,3,2-dioxaborolan-2-yl)-9H-5-oxa-9-aza-13b-boranaphtho[3,2,1-de]anthracene(9.70g,20.0 mmol), 2-bromo-N-phenylaniline(4.97 g, 20.0 mmol), K2CO3(13.1 g, 40 mmol), Pd(PPh3)4（57.75mg，5 mmol)and 120 mL a mixed solution of tetrahydrofuran and water in a ratio of four to one at 110 ℃ for overnight. The cooled mixture was extracted with a mixture of dichloromethane and water, t hen washed with dichloromethane. After removed the organic solvent, the residual solid was further purified by flash column chromatography on silica gel (eluting with petroleum ether/dichloromethane) to yield the pure product 1 as a white solid (7.89 g, 15 mmol, 75% yield).^{1}H NMR (600 MHz, C hloroform-*d*) δ 8.92 (d, *J* = 7.4 Hz, 1H), 8.72 (d, *J* = 7.7 Hz, 1H), 7.87 – 7.80 (m, 2H), 7.74 (d, *J* = 7.8 Hz, 2H), 7.61 – 7.55 (m, 2H), 7.52 – 7.42 (m, 4H), 7.32 (d, *J* = 11.2 Hz, 5H), 7.28 (s, 3H), 7.22 – 7.17 (m, 1H), 6.96 (t, *J* = 6.8 Hz, 1H), 6.86 (d, *J* = 8.7 Hz, 1H), 6.71 (d, *J* = 8.2 H z, 1H), 2.49 (s, 3H).

Synthesis of Compound 2:In a 250 mL flask charged with argon,3-methyl-9-phenyl-7-(4,4,5,5-tetram ethyl-1,3,2-dioxaborolan-2-yl)-9*H*-5-oxa-9-aza-13b-boranaphtho[3,2,1-*de*]anthracene (9.70g,20.0 mmol), 1-bromo-9*H*-carbazole (4.92 g, 20.0 mmol), K_2CO_3 (13.1 g, 40 mmol), $Pd(PPh_3)_4$ （57.75mg, 5 m

mol)and 120 mL a mixed solution of tetrahydrofuran and water in a ratio of four to one at 110 ℃ for overnight. The cooled mixture was extracted using a mixed solution of dichloromethane and water, and then washed with dichloromethane. After removed the organic solvent, the residual solid was further purified by flash column chromatography on silica gel (eluting with petroleum ether/dichloromethane) to yield the pure product 2 as a white solid (8.67g, 16 mmol, 79% yield).^{1}H NMR (600 MHz, Chloroform-*d*) δ 8.76 (s, 1H), 8.48 (s, 1H), 7.87 – 7.76 (m, 3H), 7.72 (t, *J* = 7.2 Hz, 1H), 7.48 – 7.39 (m, 3H), 7.32 (d, *J* = 16.9 Hz, 2H), 7.20 (dd, *J* = 15.6, 7.8 Hz, 4H), 7.13 (t, *J* = 7.2 Hz, 1H), 7.01 (t, *J* = 7.1 Hz, 1H), 6.90 (d, *J* = 7.5 Hz, 1H), 6.75 (d, *J* = 8.6 Hz, 1H), 6.68 (d, *J* = 8.4 Hz, 1H), 6.60 (d, *J* = 7.7 Hz, 1H), 6.38 (s, 1H), 1.56 (s, 3H).

Synthesis of Compound 3*:* In a 250 mL flask charged with argon,3-methyl-9-phenyl-7-(4,4,5,5-tetramethyl-1,3,2-dioxaborolan-2-yl)-9*H*-5-oxa-9-aza-13b-boranaphtho[3,2,1-de]anthracene(11.9g,20.0 mmol), 1-bromo-3,6-di-tert-butyl-9H-carbazole(7.14 g, 20.0 mmol), K_2CO_3 (13.1 g, 40 mmol), $Pd(PPh_3)_4$ （57.75 mg, 5 mmol) and 120 mL a mixed solution of tetrahydrofuran and water in a ratio of four to one at 110 ℃ for overnight. The cooled mixture was extracted with a mixture of dichloromethane and water, then washed with dichloromethane. After removed the organic solvent, the residual solid was further purified by flash column chromatography on silica gel (eluting with petroleum ether/dichloromethane) to yield the pure product 3 as a yellow solid (10.44g, 14 mmol, 71% yield).^{1}H NMR (600 MHz, Chloroform-*d*) δ 8.94 (s, 1H), 8.74 (d, *J* = 7.7 Hz, 1H), 8.57 (s, 1H), 8.49 (s, 1H), 8.41 (s, 1H), 8.30 (d, *J* = 8.8 Hz, 1H), 8.26 (s, 1H), 8.21 (s, 1H), 8.18 (s, 1H), 7.76 (s, 1H), 7.60 (s, 1H), 7.56 (d, *J* = 8.6 Hz, 1H), 7.51 (d, *J* = 8.3 Hz, 1H), 7.42 (s, 1H), 7.39 (d, *J* = 8.4 Hz, 1H), 7.30 (d, *J* = 7.6 Hz, 1H), 2.58 (s, 3H), 1.66 (s, 9H), 1.58 (s, 9H), 1.50 (s, 18H).

Synthesis of Target Compound BOH-BN*:* In a 120 mL sealed tube charged with argon, substrates 1 (1.05g, 2.0 mmol) and 15 mL 1,2-dichlorobenzene (*o*-DCB) were added. After adding boron bromide (5.00 g, 20.0 mmol), the tube was sealed and stirred at 220 °C for 48 h. After cooling to room temperature, the reaction was quenched by slowly adding ethanol (5.0 mL) under an ice bath. The organic solvent was concentrated under vacuum conditions. The residual solid was further purified by flash column chromatography on silica gel (eluting with petroleum ether/dichloromethane) to yield the pure product BOH-BN as a bright yellow solid (0.75 g, 1.4mmol, 64% yield).^{1}H NMR (600 MHz, Chloroform-*d*) δ 8.92 (d, *J* = 7.6 Hz, 1H), 8.71 (d, *J* = 7.8 Hz, 1H), 7.81 (t, *J* = 7.7 Hz, 2H), 7.74 (t, *J* = 8.0 Hz, 2H), 7.59 (t, *J* = 7.7 Hz, 2H), 7.51 (t, *J* = 7.9 Hz, 1H), 7.47 (d, *J* = 7.9 Hz, 3H), 7.37 – 7.29 (m, 5H), 7.28 (d, *J* = 2.5 Hz, 2H), 7.20 (t, *J* = 7.8 Hz, 1H), 6.97 (t, *J* = 7.6 Hz, 1H), 6.86 (d, *J* = 8.6 Hz, 1H), 6.71 (d, *J* = 8.3 Hz, 1H), 2.49 (s, 3H).

Synthesis of Target Compound BOH-CzBN*:* The synthesis of Compound BOH-CzBN followed the identical methodology used for Compound BOH-BN, The resulting product was a bright green solid with a yield of 67%.^{1}H NMR (600 MHz, Chloroform-*d*) δ 8.89 (s, 1H), 8.68 (d, *J* = 7.8 Hz, 1H), 8.49 (d, *J* = 8.1 Hz, 1H), 8.06 (dd, *J* = 11.2, 7.7 Hz, 2H), 8.00 (s, 1H), 7.80 (d, *J* = 7.6 Hz, 2H), 7.75 (t, *J* = 7.7 Hz, 1H), 7.65 (d, *J* = 7.8 Hz, 1H), 7.56 (s, 1H), 7.51 (t, *J* = 7.8 Hz, 1H), 7.47 – 7.42 (m, 3H), 7.38 (s, 1H), 7.32 (d, *J* = 8.4 Hz, 2H), 6.85 (d, *J* = 8.5 Hz, 1H), 5.30 (s, 1H), 2.55 (s, 3H).

Synthesis of Target Compound CzBOH-BN: The synthesis of Compound CzBOH-BN followed the identical methodology used for Compound BOH-BN, The resulting product was a bright yellow soli d with a yield of 70%.^{1}H NMR (600 MHz, Chloroform-*d*) δ 8.64 (s, 1H), 8.37 (s, 1H), 8.29 (d, *J* = 8.2 Hz, 1H), 8.11 (s, 1H), 8.05 (s, 2H), 8.00 (d, *J* = 7.5 Hz, 1H), 7.96 (s, 1H), 7.78 (s, 1H), 7. 70 (d, *J* = 8.6 Hz, 1H), 7.64 (d, *J* = 8.4 Hz, 1H), 7.48 (s, 1H), 7.19 (d, *J* = 8.5 Hz, 1H), 6.58 – 6.43 (m, 2H), 2.11 (s, 3H), 1.68 (d, *J* = 5.6 Hz, 18H), 1.58 (d, *J* = 2.6 Hz, 9H), 1.47 (d, *J* = 2.6 Hz, 9H).

3. Thermo-stability Properties

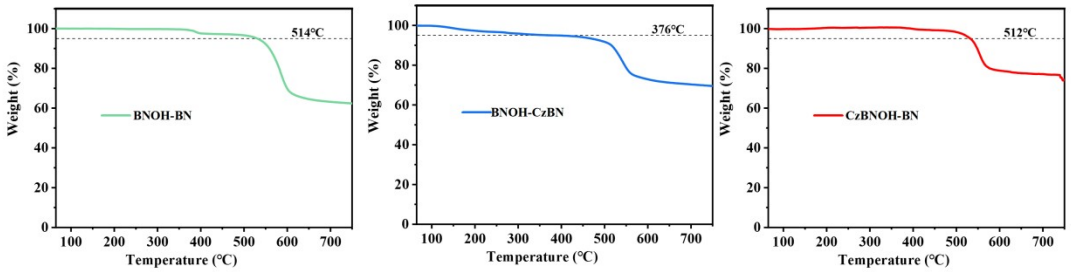

Figure S1. The thermogravimetric analysis curves of BOH-BN, BOH-CzBN, and CzBOH-BN, respectively.

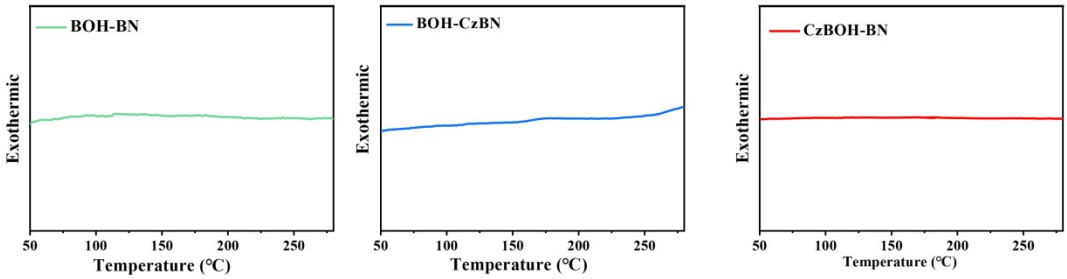

Figure S2. The differential scanning calorimetry curves of BOH-BN, BOH-CzBN, and CzBOH-BN, respectively.

4. Computational Data

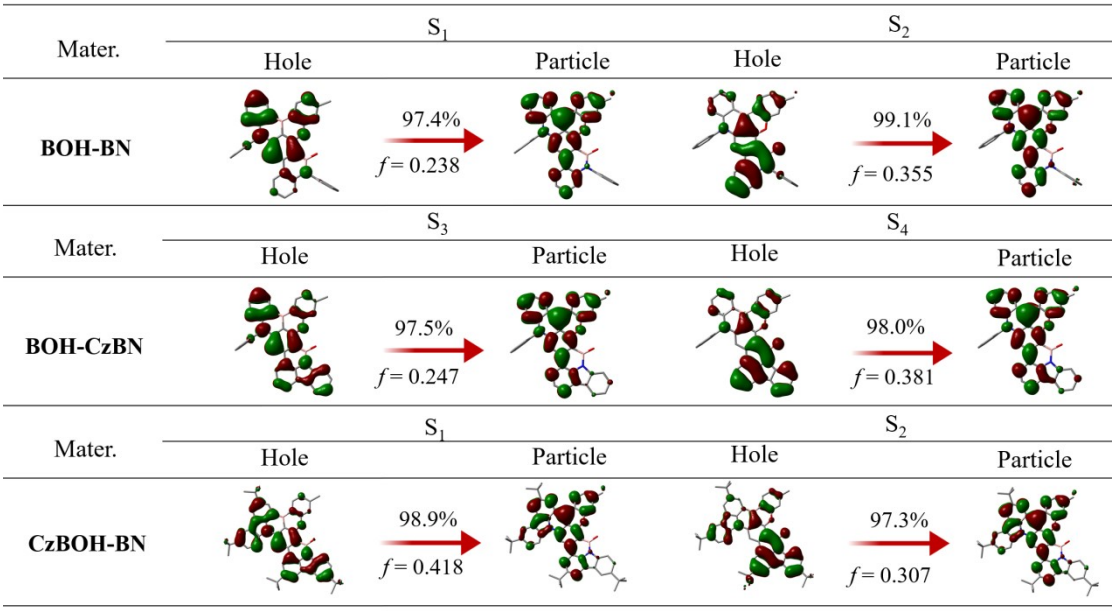

Figure S3. The natural transition orbits (NTOs) of BOH-BN, BOH-CzBN, and CzBOH-BN in S_n states ($n \leq 2$).

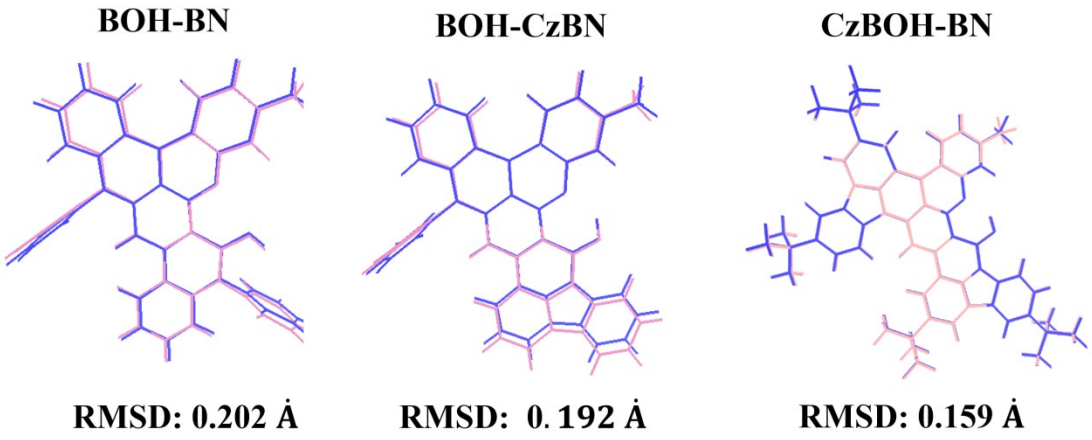

Figure S4. The calculated root-mean-square deviations (RMSDs) of BOH-BN, BOH-CzBN, and CzBOH-BN, respectively.

5. Photophysical properties

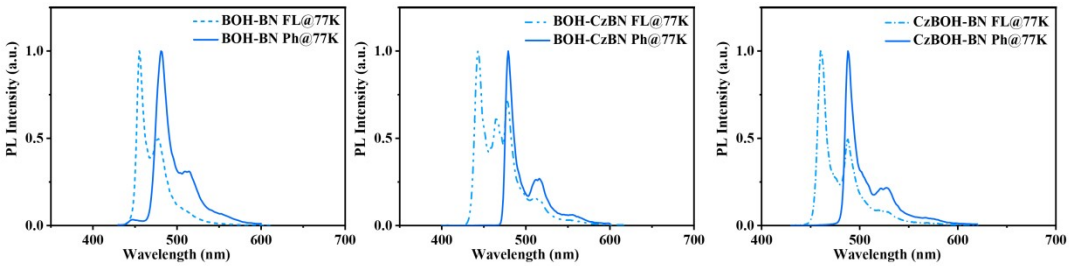

Figure S5. The low-temperature fluorescent and phosphorescent PL spectra of BOH-BN, BOH-CzBN, and CzBOH-BN in dilute toluene glasses at 77K.

Table S1. Summary of photophysical properties of BOH-BN, BOH-CzBN, and CzBOH-BN, respectively.

Emitters	T_d [a]	λ_{abs} [b]	λ_{em} [c]	HOMO [d]	LUMO [d]	S_1 [e]	T_1 [e]	ΔE_{ST} [e]
	[°C]	[nm]	[nm]	[eV]	[eV]	[eV]	[eV]	[eV]
BOH-BN	514	430	444	-5.28	-2.44	2.78	2.66	0.12
BOH-CzBN	376	429	441	-5.30	-2.43	2.85	2.63	0.22
CzBOH-BN	512	442	458	-5.31	-2.51	2.74	2.58	0.16

[a] decomposition temperature (T_d) (5% weight loss); [b] UV-vis absorption in toluene solutions at room temperature; [c] PL peaks in dilute toluene solution at room temperature; [d] experimental HOMO/LUMO determined from cyclic voltammetry and calculated of the bandgap in UV-vis absorption spectra; [d] S_1, T_1, and ΔE_{ST}s were evaluated in dilute toluene at 77 K.

Table S2. The UV-vis characteristics of BOH-BN, BOH-CzBN, and CzBOH-BN in different solvents.

Emitters	λ_{em} (nm)/FWHM (nm)				
	Hex	Tol	THF	DCM	DMF
BOH-BN	433/13	444/20	442/20	446/26	446/27
BOH-CzBN	431/12	441/17	440/17	444/27	444/33
CzBOH-BN	455/19	458/19	458/22	459/24	460/28

Table S3. Photo-physical properties of 2 wt.% BOH-BN, BOH-CzBN, and CzBOH-B in PhCzBCz films deposited using the wet process technique.

Emitters	Φ_{PL}	Φ_{PF}	Φ_{TADF}	τ_{PF}	τ_{DF}	k_r^s	k_{isc}^s	k_{risc}^s	k_{TADF}
	[%]	[%]	[%]	[ns]	[μs]	[$10^7 s^{-1}$]	[$10^7 s^{-1}$]	[$10^3 s^{-1}$]	[$10^3 s^{-1}$]
BOH-BN	51.8	45.8	6.0	9.1	24.7	5.0	6.0	9.7	4.5
BOH-CzBN	44.9	26.9	18.0	8.4	13.4	3.2	8.7	3.9	18.0
CzBOH-BN	58.9	50.4	8.5	7.3	20.0	6.9	6.8	17.0	8.5

6. Crystal properties

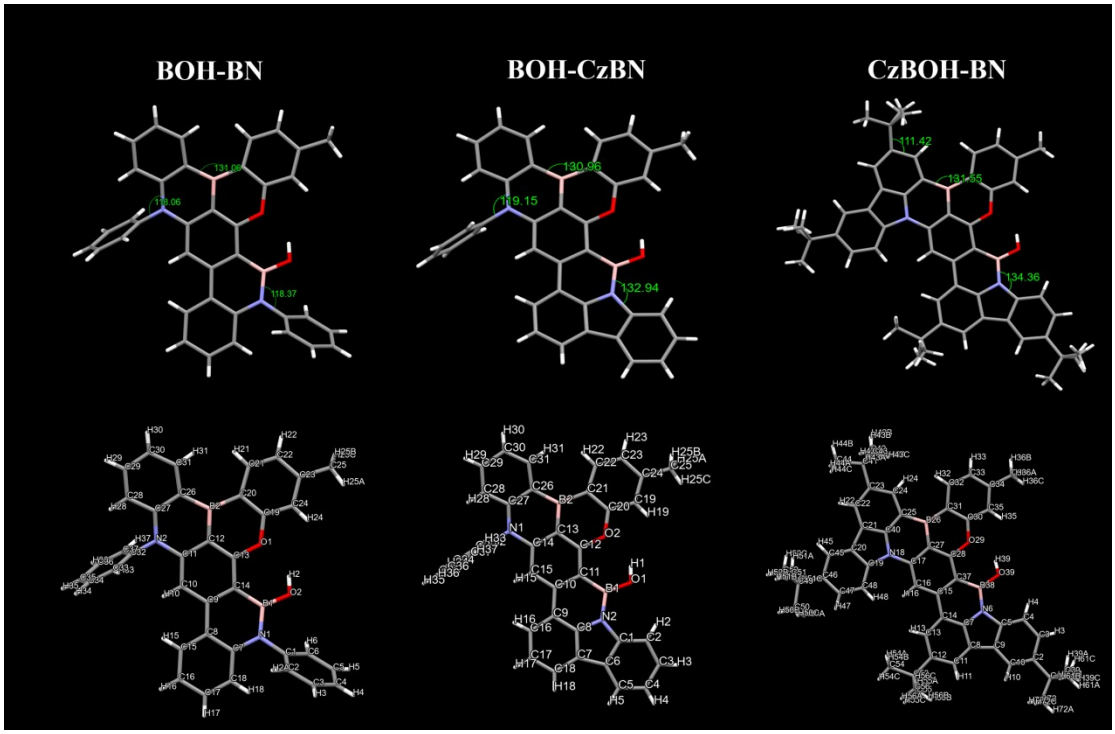

Figure S6. Schematic diagrams of the single crystal structures of BOH-BN, BOH-CzBN, and CzBOH-BN.

Table S4. Crystal data and structure refinement for BOH-BN, BOH-CzBN, and CzBOH-BN.

Identification code	BOH-BN	BOH-CzBN	CzBOH-BN
Empirical formula	$C_{37}H_{26}B_2N_2O_2$	$C_{37}H_{24}B_2N_2O_2$	$C_{53}H_{54}B_2N_2O_2$
Formula weight	552.22	550.20	772.60
Temperature/K	173	296	170
Crystal system	monoclinic	monoclinic	monoclinic
Space group	$P2_1/c$	I2/c	C2/c
a/Å	8.6738(9)	16.589(7)	36.0429(10)
b/Å	18.2010(19)	14.573(4)	21.0394(6)
c/Å	17.6365(18)	22.354(8)	44.2028(13)
α/°	90	90	90
β/°	100.186(4)	91.54(4)	104.603(2)
γ/°	90	90	90
Volume/Å^3, z	2740.4(5)	5402(3)	32437.1(16)
Density/g cm^{-3}	1.338	1.353	0.949
μ/mm^{-1}	0.082	0.083	0.432
Z	4	8	24
CCDC	2498120	2498121	2498122

7. Electrochemical measurements

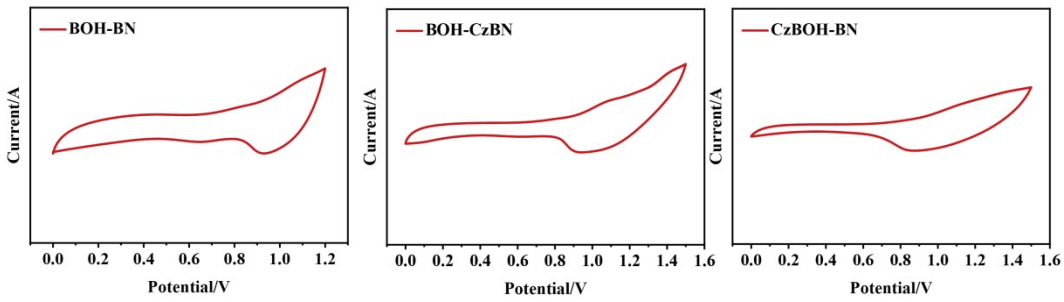

Figure S7. Cyclic voltammetry measurements of BOH-BN, BOH-CzBN, and CzBOH-BN, respectively.

Table 1. EL performance of the solution-processed OLEDs based on BOH-BN, BOH-CzBN, and CzBOH-BN with doping concentrations of 2 wt.%.

Emitters	V_{on}[(a)]	L_{max}[(b)]	CE_{max}[(b)]	PE_{max}[(c)]	EQE_{max}[(d)]	Peak[(e)]	FWHM[(e)]	CIE[(f)]
	[V]	[cd m^{-2}]	[cd A^{-1}]	[lm W^{-1}]	[%]	[nm]	[nm]	[x, y]
BOH-BN	3.6	1364	4.8	3.7	6.4	448	39	(0.14, 0.08)
BOH-CzBN	3.2	1310	4.7	3.7	5.6	446	45	(0.15, 0.09)
CzBOH-BN	3.2	1196	8.8	6.9	7.8	466	37	(0.13, 0.14)

[(a)] Measured at 1 cd m^{-2}. [(b)] Maximum luminance. [(c)] Maximum current efficiency; [(d)] Maximum power efficiency; [(e)] Peak wavelength and FWHM of the EL spectrum. [(f)] CIE coordinates.

8. NMR Spectra

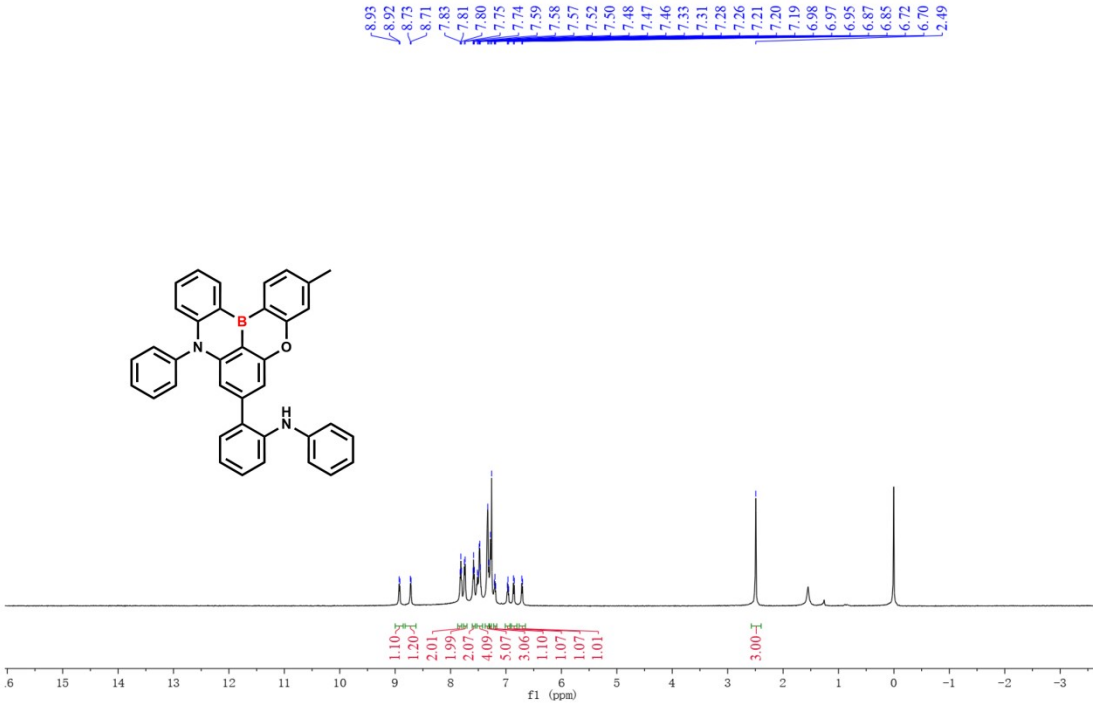

Figure S8. ^{1}H NMR spectrum of compound **1** in $CDCl_3$ solvent.

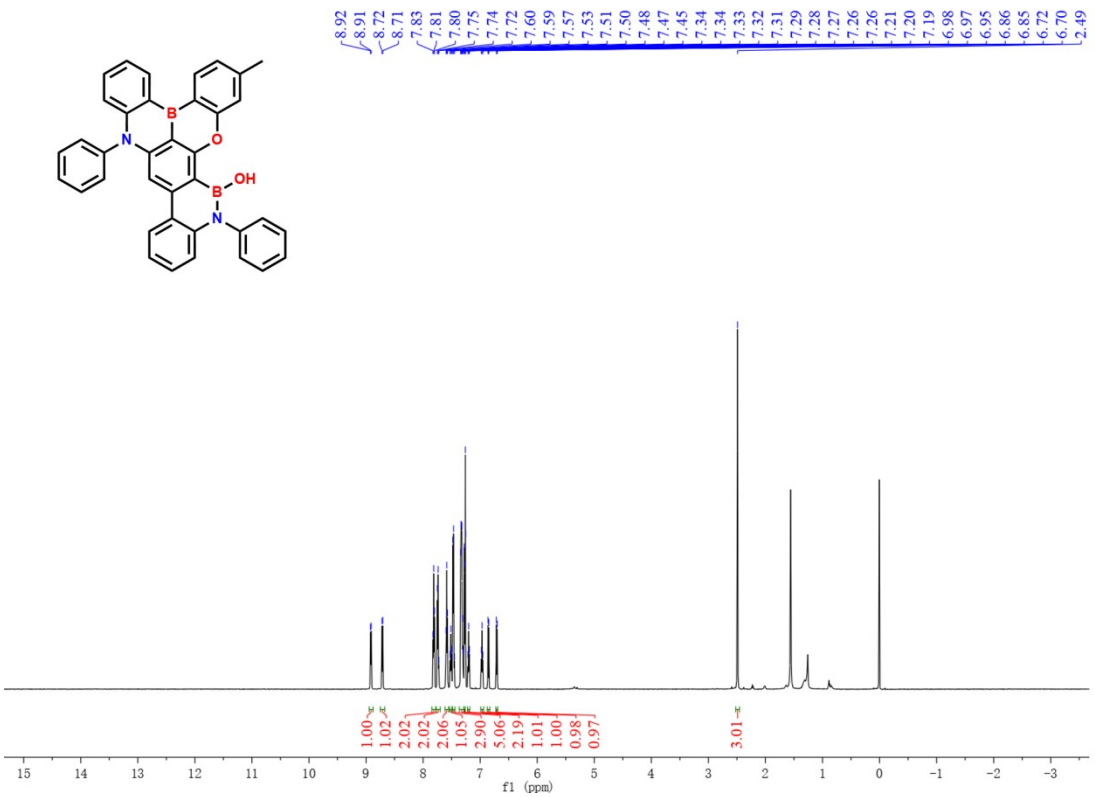

Figure S9. ^{1}H NMR spectrum of **BOH-BN** in $CDCl_3$ solvent.

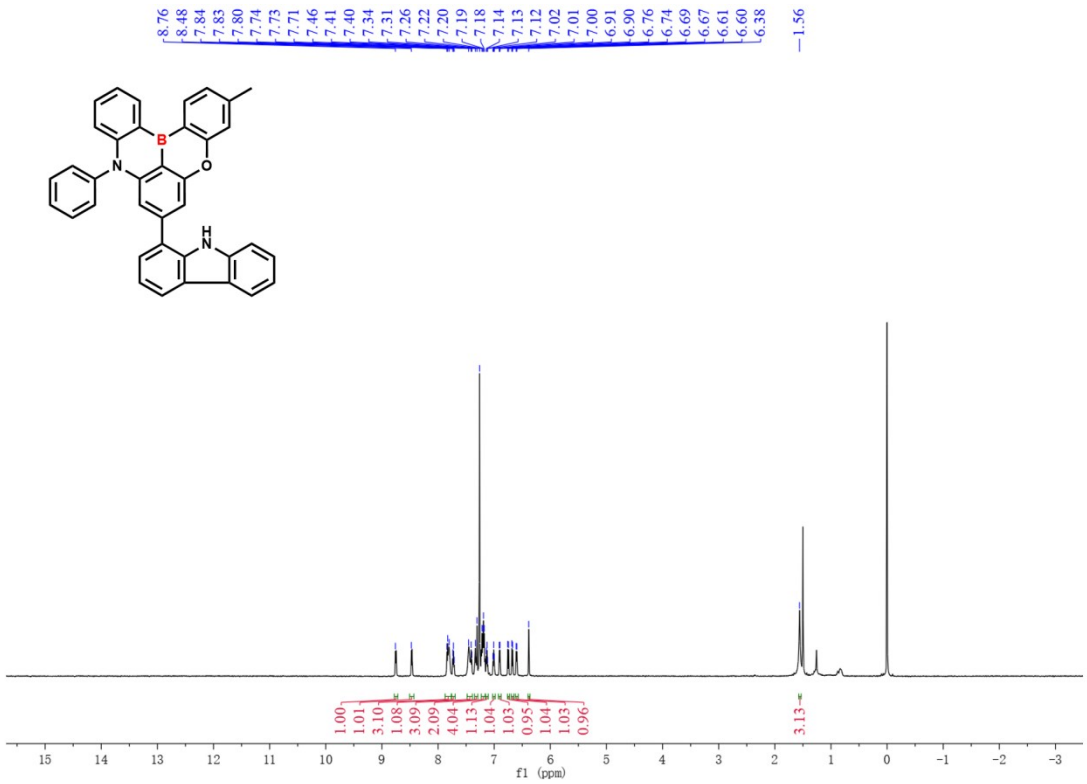

Figure S10. ^{1}H NMR spectrum of compound **2** in $CDCl_3$ solvent.

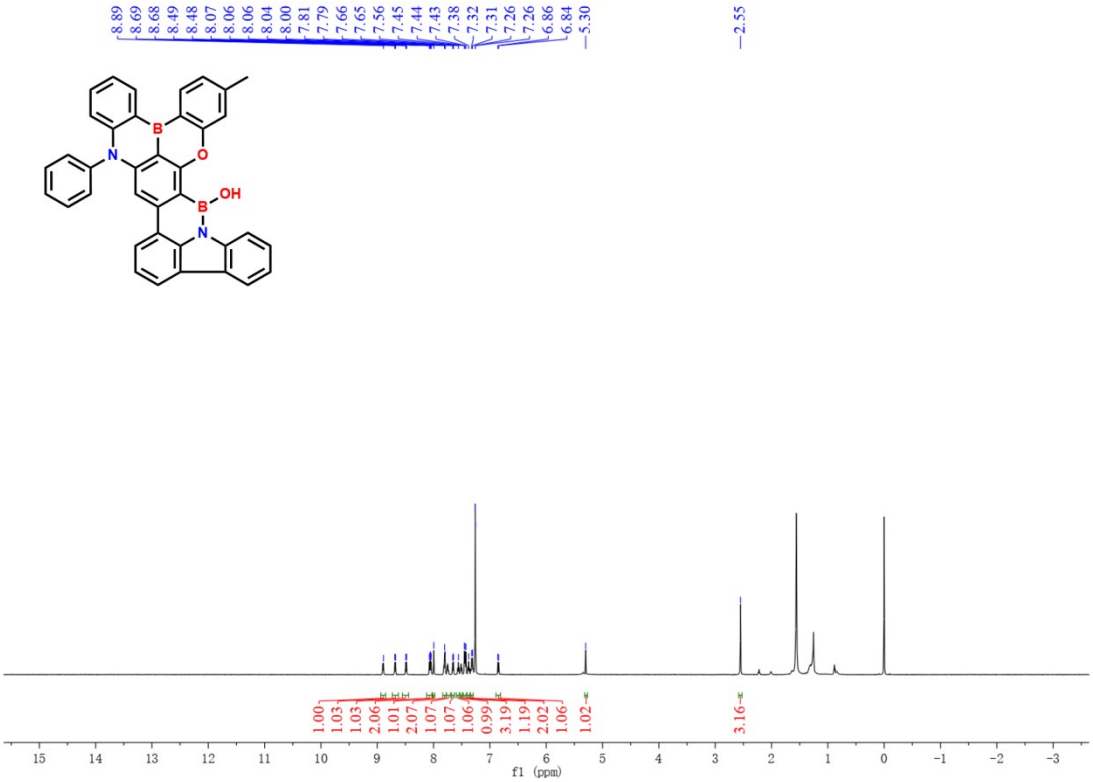

Figure S11. ^{1}H NMR spectrum of **BOH-CzBN** in $CDCl_3$ solvent.

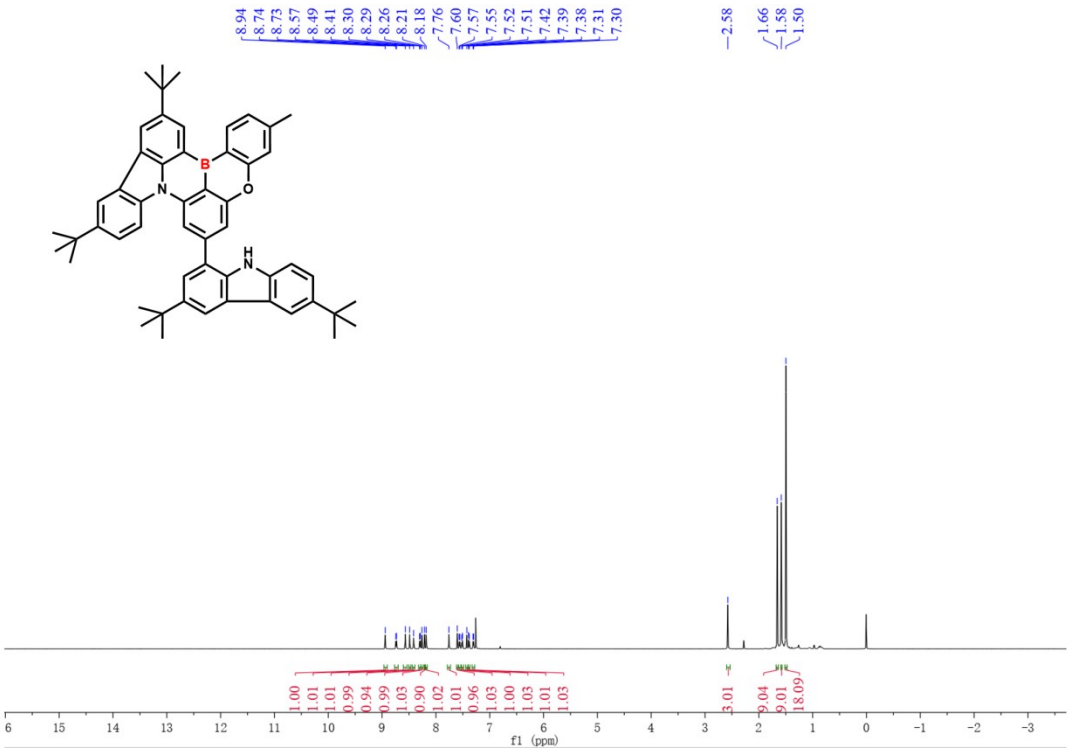

Figure S12. ^{1}H NMR spectrum of compound **3** in $CDCl_3$ solvent.

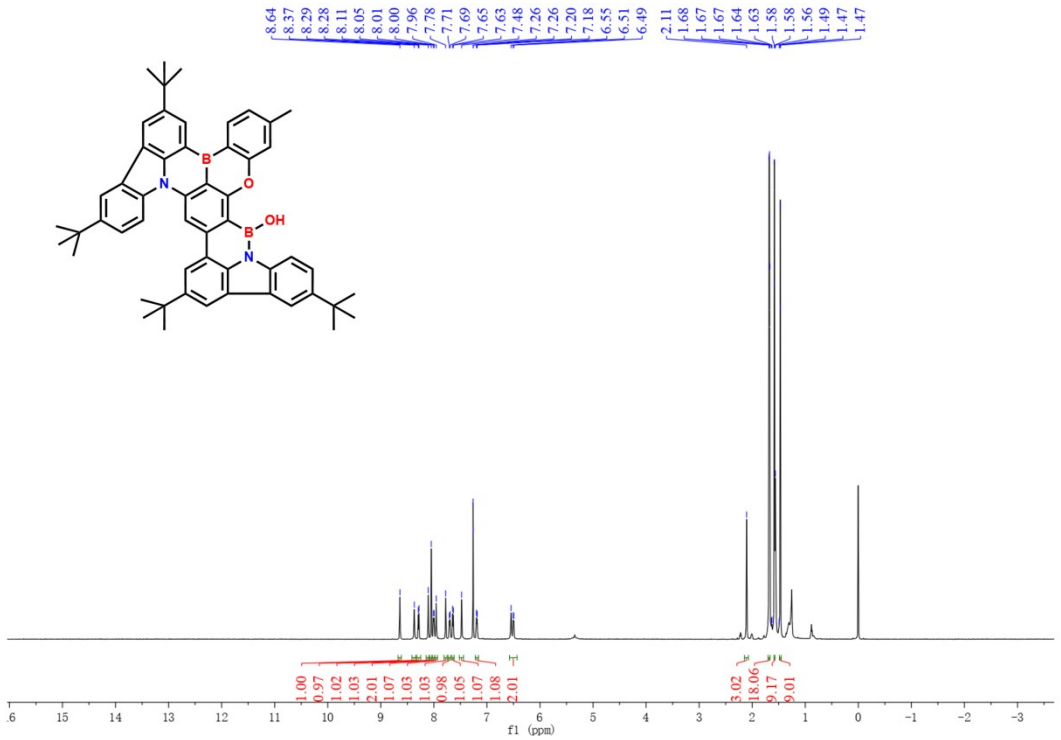

Figure S13. ^{1}H NMR spectrum of **CzBOH-BN** in $CDCl_3$ solvent.

9 · Mass spectra

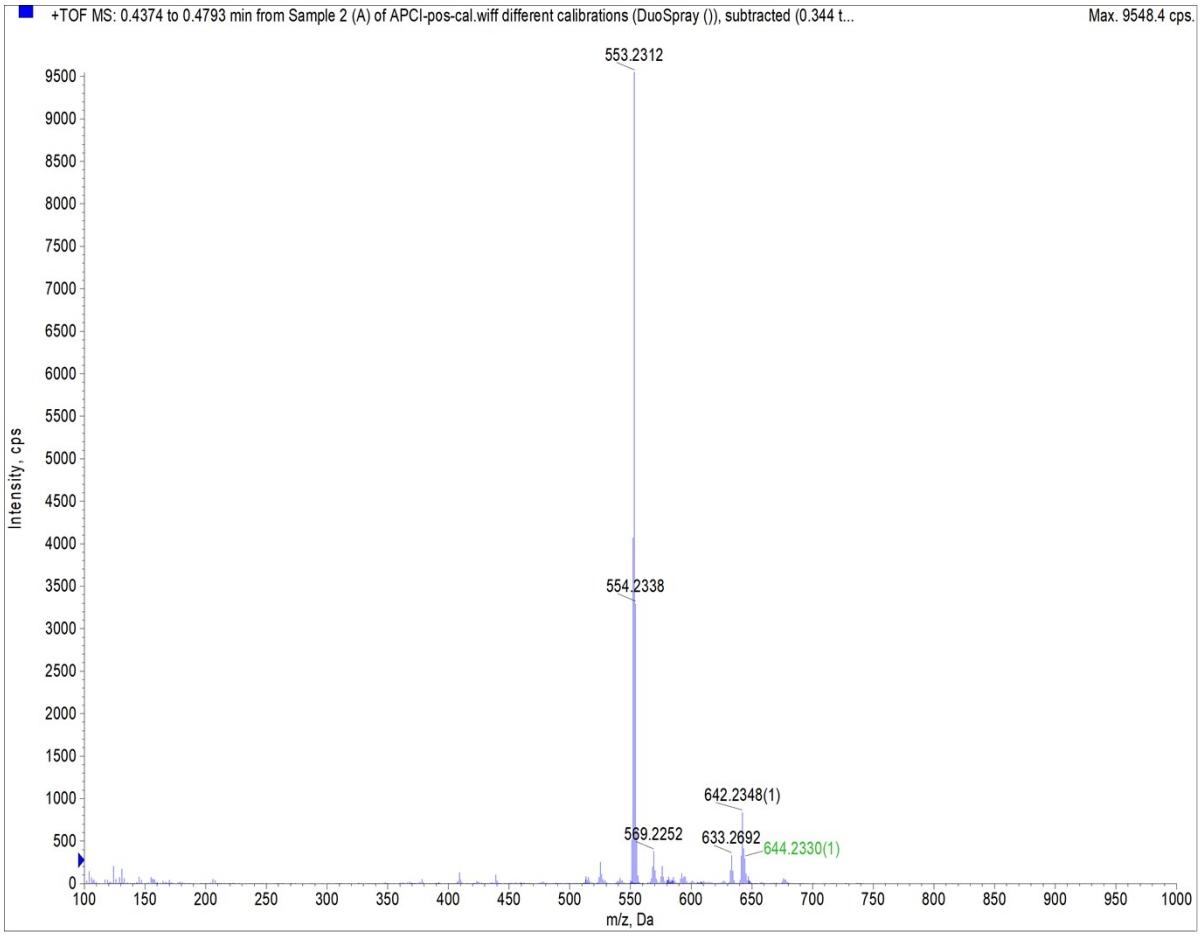

Figure S14. Mass spectra of **BOH-BN** in $CHCl_2$ solvent

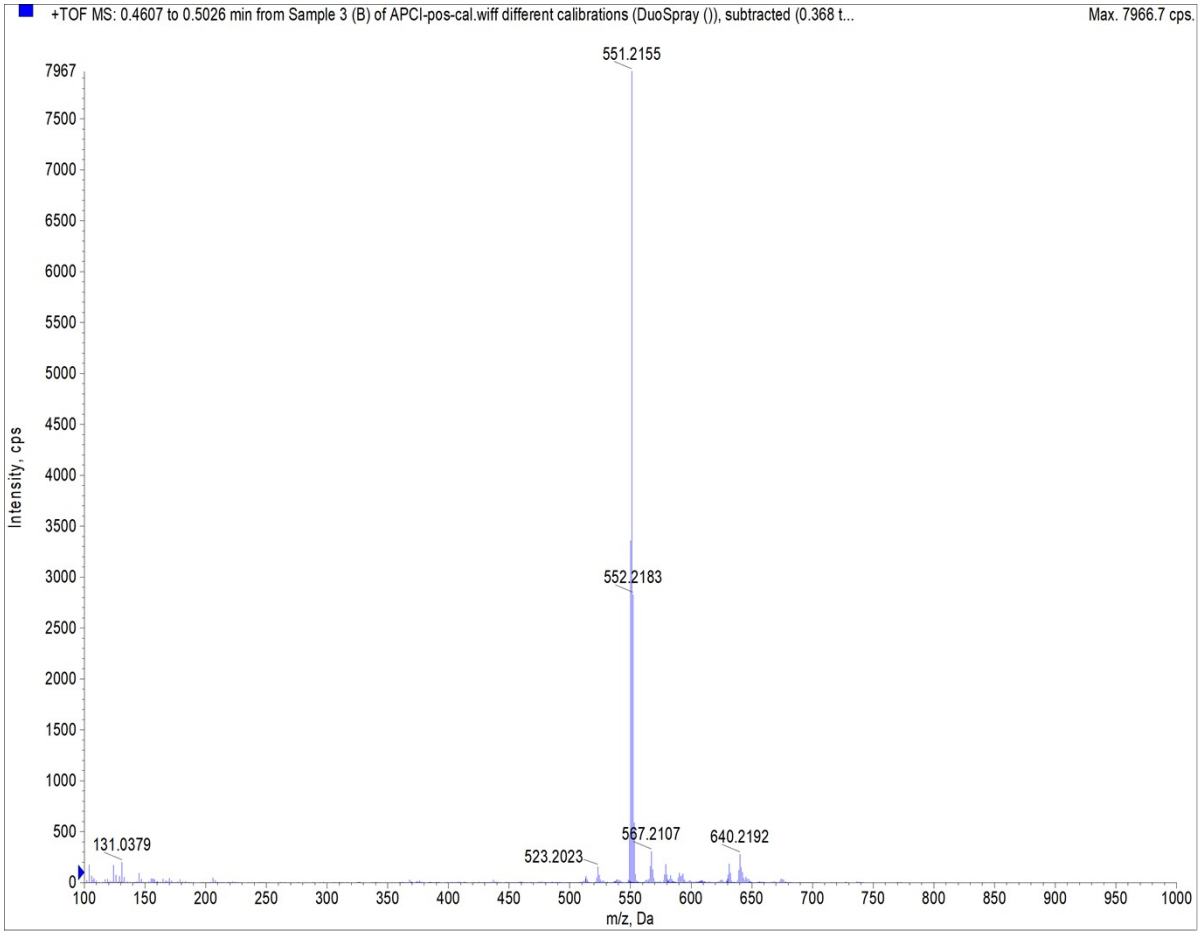

Figure S15. Mass spectra of **BOH-CzBN** in $CHCl_2$ solvent

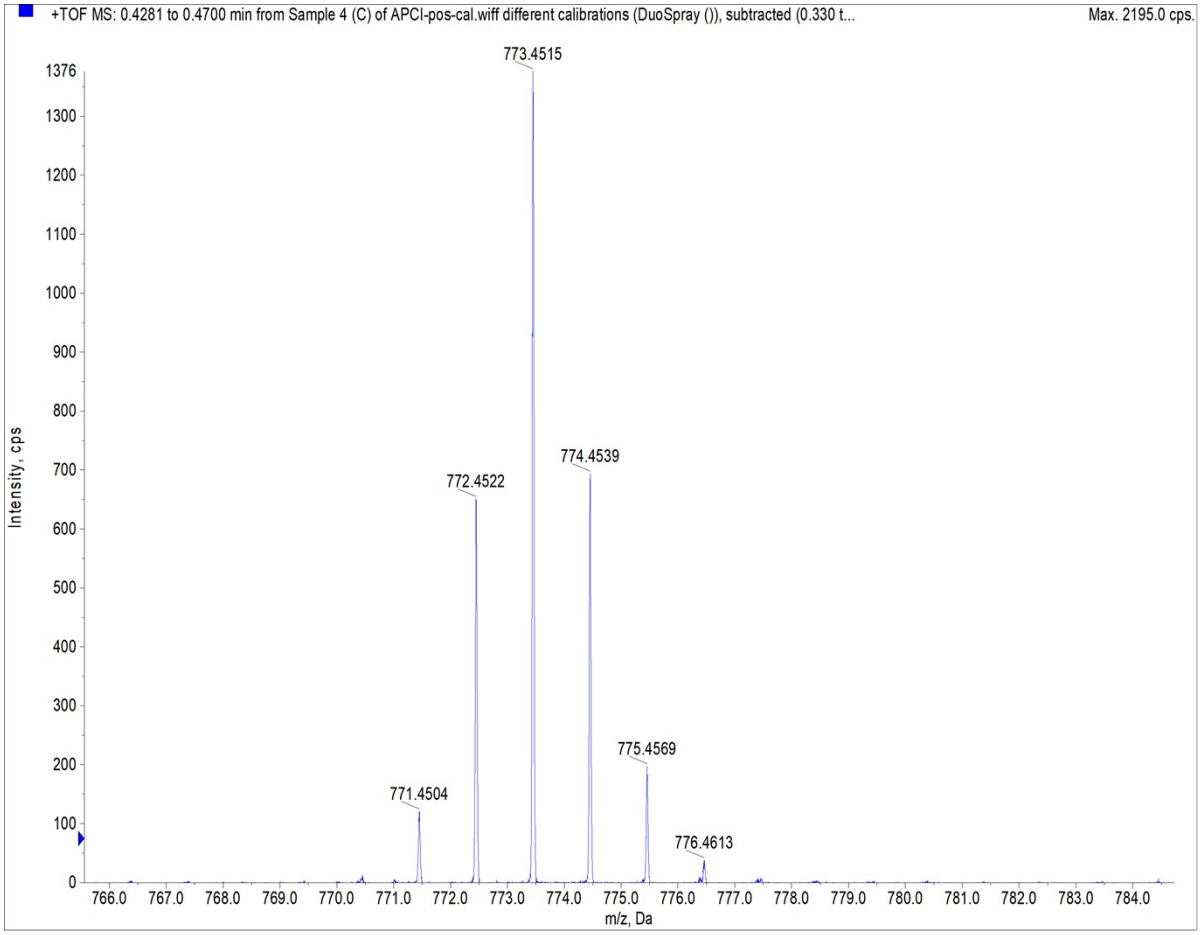

Figure S16. Mass spectra of **CzBOH-BN** in $CHCl_2$ solvent

10. Reference

[1] Frisch, M. J.; Trucks, G. W.; Schlegel, H. B.; Scuseria, G. E.; Robb, M. A.; Cheeseman, J. R.; Scalmani, G.; Barone, V.; Mennucci, B.; Petersson, G. A.; Nakatsuji, H.; Caricato, M.; Li, X.; Hratchian, H. P.; Izmaylov, A. F.; Bloino, J.; Zheng, G.; Sonnenberg, J. L.; Hada, M.; Ehara, M.; Toyota, K.; Fukuda, R.; Hasegawa, J.; Ishida, M.; Nakajima, T.; Honda, Y.; Kitao, O.; Nakai, H.; Vreven, T.; Montgomery, Jr., J. A.; Peralta, J. E.; Ogliaro, F.; Bearpark, M.; Heyd, J. J.; Brothers, E.; Kudin, K. N.; Staroverov, V. N.; Keith, T.; Kobayashi, R.; Normand, J.; Raghavachari, K.; Rendell, A.; Burant, J. C.; Iyengar, S. S.; Tomasi, J.; Cossi, M.; Rega, N.; Millam, J. M.; Klene, M.; Knox, J. E.; Cross, J. B.; Bakken, V.; Adamo, C.; Jaramillo, J.; Gomperts, R.; Stratmann, R. E.; Yazyev, O.; Austin, A. J.; Cammi, R.; Pomelli, C.; Ochterski, J. W.; Martin, R. L.; Morokuma, K.; Zakrzewski, V. G.; Voth, G. A.; Salvador, P.; Dannenberg, J. J.; Dapprich, S.; Daniels, A. D.; Farkas, O.; Foresman, J. B.; Ortiz, J. V.; Cioslowski, J.; Fox, D. J. *Gaussian 09, Revision B.01*; Gaussian, Inc.: Wallingford, CT, **2010**.

[2] X. Cai, D. Chen, K. Gao, L. Gan, Q. Yin, Z. Qiao, Z. Chen, X. Jiang, and S.-J. Su, Adv. Funct. Mater. **2018**, *28*, 1704927.

[3] W. Li, M. Li, W. Li, Z. Xu, L. Gan, K. Liu, N. Zheng, C. Ning, D. Chen, Y.-C. Wu, S.-J. Su, *ACS Appl. Mater. Interfaces,* **2021**, *13*(4), 5302-5311.